Identification of an osteopontin structural element for the restoration of a normal endometrial epidermal growth factor (EGF) profile determined by the EGF concentration on day 3 of estrous cycle and pregnancy outcome in repeat breeder dairy cows

Takashi Tanida [1], Takayoshi Tagami [2], Yojiro Yanagawa [3], and Seiji Katagiri [3,*]

[1] Laboratory of Theriogenology, Department of Clinical Sciences, Graduate School of Veterinary Medicine, Hokkaido University, Sapporo 060-0818, Japan

[2] Laboratory of Molecular Enzymology, Research Faculty of Agriculture, Hokkaido University, Sapporo 060-8589, Japan

[3] Laboratory of Theriogenology, Department of Clinical Sciences, Faculty of Veterinary Medicine, Hokkaido University, Sapporo 060-0818, Japan

*_Corresponding author_: Seiji Katagiri

E-mail address: katagiri@vetmed.hokudai.ac.jp

Postal address: Laboratory of Theriogenology, Department of Clinical Sciences, Faculty of Veterinary Medicine, Hokkaido University, Sapporo 060-0818, Japan

Abstract

The loss of a cyclic change with two peaks of increased endometrial epidermal growth factor (EGF) concentration on days 2−4 and 13−14 during the estrous cycle has been linked to low fertility in repeat breeder (RB) cows. We have shown that an intravaginal infusion of osteopontin (OPN) restored the EGF profile in RB cows. The present study aimed to determine a structural element of OPN to restore the normal EGF profile and fertility. Holstein RB cows were diagnosed the EGF profile by a single examination of the endometrial EGF concentration on day 3 of the estrous cycle. Those with an altered EGF profile were intravaginally infused with OPN and its fragments on the day of insemination (day 0); the concentration of endometrial EGF was measured on day 3, and pregnancy was diagnosed on days 30−35. In Study 1, recombinant OPN (rOPN) (16 nmol), thrombin-cleaved N- and C-terminal fragments of rOPN (N-rOPN and C-rOPN, respectively), and a combination of these fragments (Th-rOPN) were infused (n = 13−20). The restoration rate of the normal EGF profile of the N-rOPN group (25.0%) was a level in between the C-rOPN group (7.7%) and both the rOPN (55.6%) and Th-rOPN (64.3%) groups. In Study 2, PBS (n = 47), rOPN (9.5 nmol, n = 83), and peptides of integrin binding motifs, GRGDSVAYGLK (peptide 1; 32, 320, and 1,600 nmol), GRGDS (peptide 2; 320 and 1,600 nmol), and SVAYGLK (peptide 3; 320 and 1,600 nmol), were infused (n = 20−25). Restoration rates of the normal EGF profile of peptide 1 (320 and 1,600 nmol) and peptide 3 (1,600 nmol) groups (44.0−56.3%) were comparable with those of the rOPN group (63.9%) and higher than those of the PBS group (15.6%). Restoration rates of the other groups were similar to those of the PBS group. Additional cows received infusions to determine the effect on fertility. Conception rates of the peptide 1 (320 and 1,600 nmol; n = 50 each), peptide 3 (1,600 nmol; n = 55), and rOPN (n = 111) groups (41.8−50.0%) were comparable and higher than that of the PBS group (21.6%, n = 75). In Study 3, PBS (n = 24), peptide 1 (320 nmol; n = 78), and GRGESVAYGLK peptide (peptide 4; 320 and 1,600 nmol; n = 50 and 26, respectively) were infused. Restoration rates of the normal EGF profile of

peptide 4 and PBS groups (16.0−19.2%) were comparable and lower than those of the peptide 1 group (44.9%). Thus, the SVAYGLK motif may be an OPN structural element to restore the normal EGF profile and fertility in RB cows, and the RGD motif may enhance its effect.

Keywords: Repeat breeder cows, Epidermal growth factor, Osteopontin, endometrium, fertility

1. Introduction

Repeat breeder (RB) cows are defined as cows that fail to conceive after three or more inseminations without detectable abnormalities in their genital organs and estrous cycle [1,2]. The presence of RB cows is a major source of economic loss in the dairy industry because of reduced milk production and increased costs of insemination, treatment, and involuntary culling [2,3].

It is known that RB cows have low levels of circulating estradiol (E_2) [4] and progesterone (P_4) [5,6]. These hormones regulate the expression of growth factors and cytokines in the endometrium [7,8], and, thus, they could be altered in RB cows [9]. Epidermal growth factor (EGF) is one of the growth factors expressed in the endometrium [7], which has an important role in regulating endometrial function [10,11] and embryonic development [7,12]. This growth factor is synthesized in epithelial and stromal cells in the bovine endometrium [11,13,14]. The loss of the endometrial EGF peaks is related to low fertility in RB cows and postpartum cows, reviewed by Katagiri and Moriyoshi [9]. In fertile cows, the concentration of endometrial EGF exhibits a cyclic change with two peaks on days 2−4 and 13−14 during the estrous cycle. On the other hands, in approximately 70% of Holstein lactating RB cows, these EGF peaks are reduced or lost. In addition, this altered EGF profile persists between the estrous cycles in most of RB cows [9]. The concentration of endometrial EGF on day 3 of the estrous cycle has been used as an indicator of the endometrial EGF profile since the loss and recovery of the endometrial EGF peaks on day 3 coincide with those on day 14 in most cases, and could be used to diagnose abnormalities at an early stage of the estrous cycle [15].

An infusion of seminal plasma [16] and its active component, osteopontin (OPN) [17–19], into the vagina, but not the uterus, normalized the endometrial EGF profile and restored fertility in RB dairy cows. In cattle, OPN, which is also called secreted phosphoprotein 1, is an acidic protein consisting of a signal sequence and a mature region of 16 and 262 amino acids, respectively [20,21]. OPN is secreted by various tissues [22], including the ruminant reproductive organs, such as the

74 ovary [23,24], oviduct [25], uterus [26–28], testis [29], and epididymis [29]. OPN has multiple roles
75 in different physiological systems, including inflammation [30] and the reproductive system [31–
76 35]. In the reproductive system, OPN plays a role in sperm capacitation [34] and acrosome reaction
77 [32], preimplantation embryonic development [31,32], conceptus attachment [33,36,37], and corpus
78 luteum formation [35].

79 Posttranslational modifications such as phosphorylation and glycosylation have been
80 shown to be crucial for the expression of the biological activity of OPN [30,38–40]. OPN induces
81 the expression of tumor necrosis factor α (TNFα) [38] and interleukin-12 [38,40] in macrophages in
82 a phosphorylation-dependent manner in mice. Moreover, OPN promotes lung cancer cell growth in
83 humans in a glycosylation-dependent manner [39]. However, the intravaginal infusion of
84 recombinant OPN expressed in *Escherichia coli* (*E. coli*), which has no posttranslational
85 modifications [41], restored the normal endometrial EGF profile and fertility of RB dairy cows [19].
86 This indicates that these modifications were not essential, and the amino-acid sequence of OPN
87 itself may play an important role in this action of OPN in the uterus.

88 Thrombin cleavage has also been demonstrated to be crucial for the regulation of OPN
89 bioactivity [30,38,42,43]. Thrombin-cleaved OPN stimulates the migration of endothelial cells more
90 than native OPN in humans [42]. Thrombin-cleaved OPN, but not full-length OPN, induces the cell
91 migration of splenic monocytes obtained from arthritic mice [43]. The N-terminal fragment of
92 thrombin-cleaved OPN induces haptotaxis and cell spreading of macrophages, whereas the C-
93 terminal fragment induces the chemotaxis of these cells in mice [38].

94 Bovine OPN possesses one conserved thrombin-cleavage site (between Arg163 and
95 Ser164), and OPN fragments produced by thrombin treatment bind to different receptor types, such
96 as CD44 and integrins [30,44]. The C-terminal fragment of thrombin-cleaved murine OPN binds to
97 CD44, although its binding site is unknown [30,38]. The Thr121−Val140 motif of murine OPN,
98 which corresponds to Val127−Ala148 of bovine OPN, also binds to CD44 [45]. However, in bovine

OPN, there are two integrin binding motifs, including the RGD (Arg152−Asp154) and SVAYGLK (Ser155−Lys161) motifs, in the N-terminal fragment of thrombin-cleaved OPN [30,44,46]. RGD motifs are often identified as cell attachment sites for various adhesive proteins, such as fibronectin, fibrinogen, and OPN [47]. The SVAYGLK motif next to the RGD motif in bovine OPN corresponds to the SVVYGLR and SLAYGLR motifs in human and rodent OPNs, respectively [46,48]. The SVVYGLR motif in human OPN mediates interactions with integrins after thrombin cleavage [49,50]. The target receptors of the OPN RGD motif are the αvβ1, αvβ3, αvβ5, αvβ6, α5β1, and α8β1 integrins, whereas the target receptors of the SVAYGLK motif are the α4β1, α4β7, and α9β1 integrins [30,48]. In the case of human OPN, the ELVTDFPTDLPAT (Glu131−Thr143) motif, which corresponds to the bovine OPN EVDFPTDIPTI (Glu126−Ile136) motif, is also involved in α4β1 integrin binding [51].

The aim of this study is to determine a structural element of OPN to restore the normal endometrial EGF profile and fertility of RB dairy cows. We examined the effect of OPN fragments generated by thrombin treatment and synthetic peptides possessing integrin-binding OPN motifs (RGD and SVAYGLK motifs) on the restoration of the normal endometrial EGF profile and fertility in RB dairy cows.

2. Materials and methods

2.1. Preparation of recombinant OPN

Recombinant OPN (rOPN) was expressed in *E. coli* as an N-terminally His6-tagged recombinant protein of predicted mature OPN (Leu17–Asn278) and purified by Ni^{2+} affinity column chromatography, according to a previously reported method [19]. Purified rOPN was dissolved in phosphate-buffered saline (PBS) (#T9181, Takara Bio, Kusatsu, Japan) with 1% (w/v) trehalose as a cryoprotectant and filtered (pore size: 0.22 μm). In the seven batches of rOPN preparations, the purity of the rOPN was estimated to be 46.3 ± 6.0% (range: 35.9–55.5%) in the final preparation. The solutions containing 16 nmol rOPN, calculated based on the amino-acid analysis (Study 1) [52], or 9.5 nmol rOPN, calculated based on the total protein concentration, purity and the rOPN molecular weight (Study 2) [19], were aliquoted into 10 mL glass vials (NV-10, Nichiden Rika Glass, Kobe, Japan) and lyophilized. The lyophilized rOPN was stored at 4℃ until infusion into RB cows.

Our previous study found that 0.3 mg rOPN, calculated based on the total protein concentration and purity, was effective dose for the treatment for restoration of the normal endometrial EGF profile [19]. The dose of the same amount of rOPN was calculated in different methods. In study 1, this dose was equivalent to 16 nmol calculated based on the amino-acid analysis while, in study 2, this dose was equivalent to 9.5 nmol rOPN, calculated based on the total protein concentration, purity and the rOPN molecular weight.

2.2. Preparation of thrombin-cleaved rOPN

The purified rOPN (11−18 nmol/mL, calculated based on the amino-acid analysis) in PBS was treated with thrombin (2.5 IU/mL; #27084601, Cytiva, Marlborough, MA, USA) at room temperature (20–25℃) for 16 h. After adding trehalose to the reaction mixture containing the thrombin-cleaved fragments (Th-rOPN) to achieve a final concentration of 1%, the solution was

141 filtered (pore size: 0.22 μm). The solution containing the Th-rOPN that was produced by 16 nmol
142 of rOPN was aliquoted into 10 mL glass vials, lyophilized, and stored at 4℃ until infusion into RB
143 cows.
144
145 *2.3. Separation, verification, and preparation of the N- and C-terminal fragments of Th-rOPN*
146 The Th-rOPN fragments were separated using benzamidine column chromatography,
147 which is usually used to remove serine proteases, including thrombin. The Th-rOPN solution
148 containing thrombin dissolved in PBS with 0.3 M NaCl was added to a Benzamidine Sepharose 4
149 Fast Flow column (Cytiva), and the unbound fraction was collected. The bound fraction was eluted
150 with 20 mM *p*-aminobenzamidine (#01937-91, Nacalai Tesque, Kyoto, Japan).
151 N-terminal (N-rOPN) and C-terminal (C-rOPN) Th-rOPN fragments in either the bound
152 or unbound fraction separated by benzamidine column chromatography were verified by peptide-
153 mass fingerprinting (PMF) analysis [53]. Each protein band that was cut from the sodium dodecyl
154 sulfate-polyacrylamide gel electrophoresis (SDS-PAGE) gel was washed four times with 50%
155 methanol and sonication on ice, gradually dehydrated with 50 and 100% acetonitrile, and swollen
156 with 50 mM ammonium bicarbonate. Dehydration with 100% acetonitrile and swelling with 50
157 mM ammonium bicarbonate were repeated. The gel pieces were then dehydrated with 50%
158 acetonitrile containing 50 mM ammonium bicarbonate and 100% acetonitrile. The dehydrated gels
159 were dried in a vacuum. The dried gels were swollen in a trypsin solution (25 mg/mL dissolved in
160 50 mM ammonium bicarbonate) and incubated at 37°C for 19 h. Tryptic peptides were extracted
161 three times with 45% acetonitrile containing 0.1% trifluoroacetic acid and sonication on ice. The
162 extracts were dried in a vacuum and dissolved in 0.1% formic acid containing 5% acetonitrile. The
163 resultant peptides were analyzed on the nanoflow LC-MS/MS system (LTQ-OrbitrapXL;
164 ThermoFisher Scientific, Waltham, MA). The MS/MS values detected were evaluated using a
165 Mascot MS/MS ion search (https://www.matrixscience.com/).

N-terminal amino-acid sequence analysis of C-rOPN was determined by Edman degradation [54,55]. The C-rOPN was separated by SDS-PAGE and transferred to a polyvinylidene difluoride membrane (Immun-Blot PVDF Membrane, Bio-Rad Laboratories., Berkeley, California, USA) using a semi-dry transfer system. The composition of the transfer buffer was 30 mM Tris, 17 mM boric acid, 0.055% SDS, and 20% methanol. The transferred proteins were stained with 0.1% Coomassie Brilliant Blue R-250 and destained with 50% methanol. A piece of the membrane was cut out and subjected to a protein sequencer (PPSQ-53A, Shimadzu, Kyoto, Japan).

The N-rOPN and C-rOPN that were purified by the Benzamidine Sepharose 4 Fast Flow column were dissolved in PBS with 1% trehalose, filtered (pore size: 0.22 μm), and the solution containing 16 nmol N-rOPN or C-rOPN was aliquoted into 10 ml glass vials and lyophilized. Concentrations of N-rOPN and C-rOPN in the final preparations were calculated based on the amino-acid analysis. The lyophilized N-rOPN and C-rOPN were stored at 4℃ until infusion into RB cows.

2.4. Preparation of peptides

Four peptides, GRGDSVAYGLK (peptide 1), GRGDS (peptide 2), SVAYGLK (peptide 3), and GRGESVAYGLK (peptide 4), were synthesized by Peptide Institute. (Osaka, Japan). The amino-acid sequences of peptide 1, peptide 2, and peptide 3 corresponded to Gly151−Lys161, Gly151−Ser155, and Ser155−Lys161 of bovine OPN, respectively (Fig. 1). Peptide 4 shared the same sequence as peptide 1; however, aspartic acid (D) was replaced with glutamic acid (E). Peptides 1, 3, and 4 were synthesized in the form of a trifluoroacetate salt with >99.0% purity, and peptide 2 was prepared in the form of an acetate salt with >99.0% purity. The lyophilized peptides were dissolved in sterilized ultrapure water and filtered (pore size: 0.22 μm). The concentration of each peptide was determined via amino-acid analysis. Peptide samples containing 32, 320, or 1,600 nmol were aliquoted into 10 mL glass vials and lyophilized. The

lyophilized peptides were stored at 4°C until infusion into RB cows.

2.5. Determination of the concentrations of proteins and peptides

The concentrations of rOPN in the final preparations were calculated based on the amino-acid analysis [52] in Study 1 and the total protein concentration and the purity and molecular weight of rOPN [19] in Study 2. The concentrations of the other recombinant proteins or synthesized peptides in the final preparations were calculated based on the amino-acid analysis. For amino-acid analysis, the samples were hydrolyzed in 6 N HCl for 24 h at 110°C, and the amounts of resultant amino acids were measured using an L-8900 Amino-Acid Analyzer (Hitachi High-Tech, Tokyo, Japan). The concentrations of the proteins and peptides were calculated by dividing the amount of each amino acid by the number of amino acids that the protein or peptide was composed of and averaging the values.

The total protein concentration was calculated according to the estimation that the absorbance at 280 nm of 1.0 mg/mL protein is 1.0 [56], and the purity of rOPN was calculated based on densitometry of the SDS-PAGE image using ImageJ (version 1.52) (https://imagej.net/ij/index.html). For calculating the purity, purified protein solution containing 3.0 μg of total protein was separated by SDS-PAGE with 12% polyacrylamide gel at a constant watt at 3 W. Proteins were stained with Coomassie Brilliant Blue G-250 (Nacalai Tesque, Kyoto, Japan). Then, the densitometry of the gel was obtained. The purity was calculated as the proportion of areas under the curve of the target protein band to that of all protein bands. The molarity of rOPN in the final preparation was calculated by multiplying the total protein concentration and purity and dividing by the theoretical molecular weight of rOPN (31535.40).

2.6. Animals

All animal experiments were performed in accordance with the Japanese Act on

Welfare and Management of Animals. The animal use protocol was reviewed and approved by the Institutional Animal Care and Use Committee of Hokkaido University (Approval No. 19-0030). The present study was conducted from October 2021 to May 2023. Holstein lactating RB cows were housed in nine commercial farms, each of which keeps 400−1500 Holstein lactating multiparous cows, in Hokkaido, Japan. The RB cows were multiparous lactating cows (>9,500 kg of 305-day fat-corrected milk) and between two and six in parity. Cows with problems at calving and during the postpartum period requiring three or more veterinary visits were excluded from this study.

RB cows were recruited by local veterinarians according to the criteria for failure to conceive after three or more artificial inseminations (AI) without detectable abnormalities in their estrus cycle and genital organs by rectum palpation, vaginal examination, and ultrasonography or clinical signs [16,18]. The prevalence of RB cows in four farms which provided more than 90% of RB cows used in this study were between 13.0 and 18.2%. The absence of any abnormality in the uterine morphology by transrectal ultrasonography [57] and uterine cytology by cytobrush [58] were also confirmed before enrollment of study. RB cows without abnormalities in the uterine morphology and cytology was subjected to the single examination of the endometrial EGF concentration on day 3 of the estrous cycle. Those showing an altered EGF profile (between 8.6 and 12.0% in cows kept in farms) were used in the present study.

2.7. Synchronization of ovulation

Ovulation was synchronized using an Ovsynch protocol, Ovsynch protocol with E_2 treatment, or Ovsynch protocol with P_4 supplementation [59]. In the Ovsynch protocol, cows were first treated with gonadotropin-releasing hormone (GnRH) (100 μg of fertirelin acetate im; Conceral, MSD Animal Health, Tokyo, Japan), followed by prostaglandin $F_{2\alpha}$ ($PGF_{2\alpha}$) (25 mg of dinoprost tromethamine im; Pronalgon F, Zoetis Japan, Tokyo, Japan) 7 days later, and a second

241 treatment of GnRH (100 μg of fertirelin acetate im) approximately 55 ± 2 h after the $PGF_{2\alpha}$
242 treatment. In the Ovsynch protocol with E_2 treatment, estradiol benzoate (1 mg im; Estradiol
243 injection, Kyoritsu seiyaku, Tokyo, Japan) was administered one day after the $PGF_{2\alpha}$ treatment in
244 addition to the Ovsynch protocol. In the Ovsynch protocol with P_4 supplementation, controlled
245 internal drug release devices (CIDR) containing 1.9 g of progesterone (CIDR 1900; Zoetis Japan,
246 Tokyo, Japan) were inserted on the day of the first GnRH treatment in addition to the Ovsynch
247 protocol, and the CIDR was removed on the day of the $PGF_{2\alpha}$ treatment. The Ovsynch protocol
248 and the Ovsynch protocol with E_2 treatment were performed on days 5−10 or 18−20 of the estrous
249 cycle. The Ovsynch protocol with P_4 supplementation was performed on days 13−17 of the estrous
250 cycle. The day following the second GnRH treatment was considered day 0.
251
252 *2.8. Endometrial tissue collection, EGF assay, and analysis of the endometrial EGF profile*
253 Endometrial tissues were collected using a biopsy instrument (Fujihira Industry,
254 Tokyo, Japan) with caudal epidural anesthesia (4–5 mL of 2% lidocaine and 2% xylocaine;
255 Fujisawa Pharmaceutical, Osaka, Japan), as previously reported [60]. Tissues of the intercaruncle
256 regions that consist of the epithelial cells and the stratum compactum were weighed and frozen in
257 liquid nitrogen within 10 min of collection and stored at −20℃ or −30℃ until the EGF assay.
258 Endometrial tissues were processed, and EGF was extracted from the tissue
259 homogenate, as previously described [61]. The efficiency of the extraction from the tissue
260 homogenate was 88-100%. The EGF concentrations in the tissue extracts were determined using a
261 double-antibody sandwich enzyme immunoassay in duplicates, as previously reported [16]. An
262 anti-human EGF mouse monoclonal antibody (#MAB636, R & D Systems, Minneapolis, MN,
263 USA) and an anti-human EGF rabbit antiserum (#5022-100, Biogenesis, Poole, UK) were used as
264 the solid-phase antibody and detection antibody, respectively. The assay system was verified for
265 the measurement of bovine EGF using recombinant bovine EGF [16], and the assay sensitivity was

established as 10 pg/well. The intra- and inter-assay coefficients of variation at 50 pg/well were 4.2% and 6.8%, respectively.

In the present study, the endometrial EGF profile was considered to be normal when the endometrial EGF concentration was within the normal range for day 3 (4.70−13.50 ng/g tissue weight), while the EGF profile was judged as altered when the EGF concentration was lower than 4.70 ng/g tissue weight [61,62].

2.9. AI and infusion of samples into the vagina

AI was performed using commercial frozen-thawed Holstein semen by professional AI technicians within 16–20 h after the second GnRH treatment of the Ovsynch protocols for ovulation synchronization.

All OPN treatment samples were dissolved in 10 mL of PBS, loaded into a 10 mL syringe, and infused into the vagina immediately after AI, as previously described [16,18]. Briefly, the tip of a disposable plastic AI catheter, which was attached to the syringe loaded with the OPN treatment sample, was introduced into the vagina and guided into the vagina, adjacent to the external orifice of the cervix. The plunger was then depressed to deposit the sample.

2.10. Study design

2.10.1. Study 1

The effect of Th-rOPN, N-rOPN, and C-rOPN treatment on the restoration of the normal endometrial EGF profile was evaluated. RB cows with an altered endometrial EGF profile (n = 65) were used for this study (Fig. 2). RB cows were synchronized for ovulation with either the Ovsynch protocol, Ovsynch protocol with E_2 treatment, or Ovsynch protocol with P_4 supplementation and underwent AI. Cows were randomly assigned to four groups with 16 nmol of rOPN (n = 18), N-rOPN (n = 20), and C-rOPN (n = 13), as well as Th-rOPN produced by 16 nmol

291 of rOPN (n = 14) that was infused into the vagina immediately after AI. The endometrial EGF
292 concentration was determined on day 3 for the second time. Pregnancy was diagnosed by
293 transrectal ultrasonography on days 30−35 after AI.
294
295 *2.10.2. Study 2*
296 The effects of OPN peptides on the restoration of the normal endometrial EGF profile and
297 fertility were examined using 431 RB cows. The timeline of the study was the same as that of
298 Study 1. RB cows with an altered endometrial EGF profile were synchronized for ovulation. The
299 cows were then infused with treatment samples into the vagina immediately after AI. Study 2 was
300 conducted in two trials. In trial 1, one of the following samples was randomly infused into the
301 vagina in RB cows to examine the effects of those samples on the normalization of the endometrial
302 EGF profile: PBS (negative control; n = 45), rOPN (positive control, 9.5 nmol; n = 83), peptide 1
303 (32, 320, and 1,600 nmol; n = 25 each), peptide 2 (320 and 1,600 nmol; n = 20 each), or peptide 3
304 (320 and 1,600 nmol; n = 25 and 23, respectively). In trial 2, additional RB cows were infused into
305 the vagina with PBS (n = 30), rOPN (n = 28), peptide 1 (320 and 1,600 nmol; n = 25 each), or
306 peptide 3 (1,600 nmol; n = 32) to investigate the effect on fertility with an increased number of
307 animals.
308
309 *2.10.3. Study 3*
310 The effect of peptide 4 on the restoration of the normal endometrial EGF profile was
311 examined to clarify the role of the RGD motif. The timeline of the study was the same as that of
312 Study 1. RB cows with an altered endometrial EGF profile were synchronized for ovulation by
313 using the Ovsynch protocol and infused with PBS (negative control; n = 24), 320 nmol peptide 1
314 (positive control; n = 78), or peptide 4 (320 and 1,600 nmol; n = 50 and 26, respectively) into the
315 vagina immediately after AI.

316

317 *2.11. Data analyses*

318 Endometrial EGF concentrations before and after treatment were compared using
319 Wilcoxon signed-rank test. Endometrial EGF concentrations of the peptide 1, peptide 2, and
320 peptide 3 groups in trials 1 and 2 of Study 2 were compared to those of the negative (PBS) and
321 positive (rOPN) control groups using Steel test. Endometrial EGF concentrations between the
322 negative and positive control groups in trials 1 and 2 of Study 2 were compared using Wilcoxon
323 rank sum test. Endometrial EGF concentrations between groups in Study 1, the total of trials 1 and
324 2 of Study 2, and Study 3 were compared using Steel–Dwass test.

325 The proportion of cows with a normal endometrial EGF profile after treatment
326 (restoration rates) and the conception rates of each of the peptide 1, peptide 2, and peptide 3
327 groups in trials 1 and 2 of Study 2 were compared to those of the negative and positive control
328 groups using Fisher's exact test with the Benjamini–Hochberg method. Restoration and conception
329 rates between the negative and positive control groups in trials 1 and 2 of Study 2 were compared
330 using Fisher's exact test. The restoration and conception rates between the groups in Study 1, a
331 total of trials 1 and 2 of Study 2, and Study 3 were compared using Fisher's exact test with the
332 Benjamini–Hochberg method.

333 Wilcoxon signed-rank test, Steel test, Wilcoxon rank sum test, Steel–Dwass test, and
334 Fisher's exact test were performed using the computer software JMP Pro 16 (SAS Institute, Tokyo,
335 Japan). The P-values in Fisher's exact test were adjusted for multiple comparisons using the
336 Benjamini–Hochberg method [63].

337 Two cows infused with rOPN, two cows infused with Th-rOPN, and one cow infused
338 with C-rOPN were culled before the pregnancy diagnosis in Study 1. One cow infused with PBS,
339 two cows infused with rOPN, and one cow infused with 320 nmol peptide 2 were culled before the

pregnancy diagnosis in trial 1 of Study 2. Thus, conception rates were analyzed after excluding their data. A P value < 0.05 was considered statistically significant.

342 **3. Results**

343 *3.1. Verification and preparation of Th-rOPN, N-rOPN, and C-rOPN*

344 Recombinant OPN expressed in *E. coli* was observed as a band via SDS-PAGE with an
345 apparent molecular mass of 47.7 × 10^3 (Fig. 3A and 3B, lane 2). The band corresponding to
346 rOPN disappeared, and two bands with apparent molecular masses of approximately 33.7 × 10^3
347 and 20.2 × 10^3 appeared as major bands via SDS-PAGE analysis in Th-rOPN (Fig. 3A, lane 3).
348 The two fragments in the Th-OPN were separated by benzamidine column chromatography (Fig.
349 3B, lane 3 and 4), and their tryptic peptide masses matched with the theoretical masses calculated
350 from the amino-acid sequences of the N- or C-terminal ends of the putative thrombin-cleavage site
351 (Arg163−Ser164 [44]) of rOPN (Fig. 3C). Furthermore, the N-terminal amino-acid sequence of the
352 20.2 × 10^3 fragment (Fig. 3B, lane 4) was SKKFRRS, which corresponds to the bovine OPN
353 region of Ser164−Ser170 (Fig. 3C). Based on these results, we concluded that the two fragments
354 generated by the thrombin treatment of rOPN were N-rOPN and C-rOPN, even though the C-
355 terminal amino-acid sequence of the N-rOPN could not be determined by PMF analysis. In two
356 batches of N-rOPN (Fig. 3B, lane 3) and C-rOPN preparations (Fig. 3B, lane 4), the bands of N-
357 rOPN accounted for 85.6 and 93.3% in the first and second batches, respectively, while those of C-
358 rOPN accounted for 73.3 and 79.4%, respectively, of the total protein content in the final
359 preparation in the gel image of SDS-PAGE.

360

361 *3.2. Study 1: Effect of Th-rOPN, N-rOPN, and C-rOPN on the restoration of the normal*
362 *endometrial EGF profile*

363 Endometrial EGF concentrations before treatment were comparable between all of the
364 groups (Fig. 4). The endometrial EGF concentrations after treatment became higher than those
365 before treatment in the rOPN, Th-rOPN, and N-rOPN groups, whereas the endometrial EGF
366 concentrations before and after treatment were comparable in the C-rOPN group. Endometrial

EGF concentrations after treatment in both Th-rOPN and N-rOPN groups were comparable, and they were at an intermediate level between the rOPN and C-rOPN groups ($P < 0.05$). Endometrial EGF concentrations after treatment in the C-rOPN group were lower than those in the rOPN group.

Restoration rates of the normal endometrial EGF profile of the rOPN and Th-rOPN groups were comparable and higher than those of the C-rOPN group ($P < 0.05$) (Table 1). The restoration rate of the N-rOPN group was a level in between the rOPN and C-rOPN groups ($P < 0.05$).

3.3. Study 2: Effects of OPN peptides on the restoration of the normal endometrial EGF profile and fertility

In trial 1, the endometrial EGF concentrations before treatment were comparable in all of the groups (Fig. 5A). The endometrial EGF concentrations after treatment (Fig. 5A) and the restoration rates of the normal endometrial EGF profile (Table 2) of the 320 nmol and 1,600 nmol peptide 1 and the 1,600 nmol peptide 3 groups were higher than those of the PBS group ($P < 0.05$), and they were comparable to those of the rOPN group. The endometrial EGF concentrations after treatment and the restoration rates of the normal endometrial EGF profile of the 320 nmol and 1,600 nmol peptide 2 and the 320 nmol peptide 3 groups were lower than those of the rOPN group ($P < 0.05$), and they were similar to those of the PBS group. Endometrial EGF concentrations after treatment with 32 nmol peptide 1 were higher than those of the PBS group ($P < 0.05$), and they were comparable to those of the rOPN group. However, the restoration rate of the normal endometrial EGF profile of the 32 nmol peptide 1 group remained comparable to that of the PBS group and lower than that of the rOPN group ($P < 0.05$).

In trial 2, the endometrial EGF concentrations before treatment were comparable in all of the groups (Fig. 5B). The endometrial EGF concentrations after treatment in the 320 nmol and 1,600 nmol peptide 1 group were comparable to those of the rOPN group and higher than those of

392 the PBS group ($P < 0.05$). Endometrial EGF concentrations after treatment in the 1,600 nmol
393 peptide 3 group were similar to those of the rOPN and PBS groups. The restoration rates of the
394 normal endometrial EGF profile and conception rates of each group in trial 2 are shown in Tables 2
395 and 3, respectively.
396 In the total of the two trials, the endometrial EGF concentrations before treatment were
397 comparable in all of the groups (Fig. 5C). The endometrial EGF concentrations after treatment
398 (Fig. 5C) and the restoration rates of the normal endometrial EGF profile (Table 2) of the 320 nmol
399 and 1,600 nmol peptide 1 and 1,600 nmol peptide 3 groups were comparable to the rOPN groups
400 and higher than those of the PBS group ($P < 0.05$). In cows with the normalized endometrial EGF
401 profile after treatment, the endometrial EGF concentrations after treatment in the 320 nmol and
402 1,600 nmol peptide 1 groups were comparable to those of the rOPN group and higher than those of
403 the PBS group ($P < 0.05$). While those after treatment in the 1,600 nmol peptide 3 groups reached
404 an intermediate level between the PBS and rOPN groups and were comparable to all other groups
405 (Fig. 5C). The conception rates in cows with a normalized endometrial EGF profile were higher
406 than those in cows whose endometrial EGF profile had not achieved normalization in each group
407 ($P < 0.05$) (Table 3). Furthermore, the conception rates of the 320 nmol and 1,600 nmol peptide 1
408 and 1,600 nmol peptide 3 groups were comparable to those of the rOPN group and higher than
409 those of the PBS group ($P < 0.05$).
410
411 *3.4. Study 3: Effect of peptide 4 on the restoration of the normal endometrial EGF profile*
412 Before treatment, the endometrial EGF concentrations of the 1,600 nmol peptide 4 group
413 were higher than those of the PBS group ($P < 0.05$), while those of the 320 nmol peptide 1 and 320
414 nmol peptide 4 groups were comparable to the PBS group (Fig. 6). After treatment, the
415 endometrial EGF concentrations of the 1,600 nmol peptide 4 group were comparable to those of
416 the 320 nmol peptide 1 group and higher than those of the PBS group ($P < 0.05$). The endometrial

417 EGF concentrations of the 320 nmol peptide 4 group were at an intermediate level between the 320
418 nmol peptide 1 and PBS groups. The restoration rates of the normal endometrial EGF profiles of
419 the 320 nmol and 1,600 nmol peptide 4 groups were comparable to those of the PBS group and
420 lower than those of the 320 nmol peptide 1 group ($P < 0.05$) (Table 4).

421 **4. Discussion**

422 In this study, we demonstrated that the SVAYGLK peptide (peptide 3) is a minimal
423 element of OPN that is required to restore the normal endometrial EGF profile in RB cows.
424 Although the RGD is not essential for the activity of OPN to normalize the endometrial EGF
425 profile, the addition of the RGD motif to the N-terminal end of peptide 3 (GRGDSVAYGLK,
426 peptide 1) enhances the effect of peptide 3. In addition, the results showed that normalization of
427 the endometrial EGF profile by peptides 1 and 3 led to improved fertility.

428 Interestingly, the replacement of aspartic acid (D) in RGD motif to glutamic acid (E)
429 diminished the effect of peptide 1 to the control (PBS) levels. Similarly, it has been reported that
430 the replacement of the RGD motif of OPN with RGE resulted in a decrease in the effect of OPN on
431 cell adhesion that is mediated by α9β1 integrin, which is a target receptor of the SVVYGLR motif
432 homologs to bovine SVAYGLK, in human melanoma cells [64].

433 In cattle, OPN binds to integrins via the RGD (Arg152−Asp154) and SVAYGLK
434 (Ser155−Lys161) motifs of the N-terminal fragment that is generated by thrombin cleavage
435 [44,46,48], although the ELVTDFPTDLPAT (Glu131−Thr143) motif of human OPN, which
436 corresponds to the EVDFPTDIPTI (Glu126−Ile136) motif of bovine OPN, has also been described
437 as an integrin binding site [51]. In addition, OPN binds to CD44 via an unknown binding site on
438 the C-terminal fragment that is generated by the thrombin cleavage [38,40] and via the
439 Thr121−Val140 of murine OPN, which corresponds to the Val127−Ala148 of bovine OPN [45].
440 The target receptors of the SVAYGLK motif are the α4β1, α4β7, and α9β1 integrins [30,48] and,
441 thus, the interaction between this motif and these integrins may be responsible for the OPN
442 activity to normalize the endometrial EGF profile in RB cows. Therefore, information on the
443 expression of these integrins in the vagina during the estrous cycle, especially at estrus, may
444 provide further understanding of the receptive mechanism of OPN and the potential application of
445 treatment using OPN or its partial peptides.

446 Some functions of OPN need posttranslational modifications such as glycosylation and
447 phosphorylation for its expression [38–40], whereas other functions do not require [36,37,65]. In
448 sheep and pigs, recombinant rat OPN without posttranslational modifications promote
449 trophectoderm cell adhesion and migration [36,37] and ion transport across the placenta [65]. Our
450 previous [19] and present results also suggested that OPN does not require the posttranslational
451 modifications to exert the restoration of the normal endometrial EGF profile. Indeed, α4 integrin,
452 which is a target receptor of the SVYAGLK motif, bind to OPN independently of the
453 posttranslational modifications [66]. However, it is unknown whether these posttranslational
454 modifications enhance and stabilize the function of OPN to restore the normal EGF profile in RB
455 cows.
456 Although the mechanisms by which OPN normalized the endometrial EGF profile are
457 unknown, the site of action of OPN for the restoration of the normal endometrial EGF profile in
458 RB cows has been thought to be the vagina [16,18,19]. Seminal plasma, which contains OPN,
459 restored the normal endometrial EGF profile and fertility by infusion into the vagina and not the
460 uterus in RB cows [16]. It has also been reported that intrauterine infusions of seminal plasma at
461 the time of AI failed to improve fertility in beef [67] and dairy cows [67,68]. In addition, during
462 natural mating, seminal plasma ejaculated into the vagina could not reach the uterus [69] because
463 of the low volume of semen ejaculated by the bull [70], the length of the cervix [71], and the high
464 viscosity of cervical mucus [72].
465 OPN activates immune cells, including macrophages, dendritic cells, and lymphocytes,
466 and induces a pro-inflammatory response [30]. Endometrial functions are regulated by pro-
467 inflammatory cytokines, such as interleukin-6 (IL-6) [73] and TNFα [74]. Therefore, it can be
468 hypothesized that OPN activates immune cells in the vagina, and these cells enter the adjacent
469 lymph node via lymph, thus causing further immune cell activation in the lymph nodes [18,19].
470 The activated immune cells in the vagina and lymph nodes then infiltrate into the uterus via lymph

471 and blood circulation. This may, in turn, normalize the endometrial EGF profile in RB cows. In
472 particular, TNFα produced by activated immune cells has been hypothesized to be involved in the
473 restoration of the normal endometrial EGF profile by OPN treatment [18] since TNFα activates
474 receptor signaling pathways of estrogen, which is a primary regulator of EGF synthesis in
475 endometrial epithelial cells [7,74,75]. In support of this hypothesis, the SLAYGLR motif, the
476 mouse homolog of the SVAYGLK motif, mediates pro-inflammatory responses by OPN in mice
477 [43,76]. OPN induces a pro-inflammatory response via the SLAYGLR motif in rheumatoid
478 arthritis [43] and inflammatory bowel disease [76] murine models. The receptive mechanism of the
479 SVAYGLK motif in the vagina and immune cells needs to be investigated in cows to confirm the
480 hypothesis.
481 The interaction between OPN and integrin expressed in the conceptus and endometrium
482 have known to have important roles in mammalian pregnancy [77]. At the phase of the conceptus
483 attachment, OPN directly promote adhesion and migration of trophectoderm cells to uterine
484 luminal epithelial cells via integrins expressed in these cells [77]. In addition, it has been assumed
485 that integrins may utilize other signaling cascades within the integrin adhesome to influence the
486 uterine-placental environment [65,77,78]. OPN affect angiogenesis [78] and ion transport [65] in
487 porcine uterine and placental tissue via integrins. However, it seems unlikely that OPN infused
488 into the vagina directly affect the uterus in cows and we hypothesized that OPN may act as
489 cytokine which utilizes integrin signal cascade as discussed above.
490 This study demonstrated that the infusion of N-rOPN alone had a lower effect on the
491 normalization of the endometrial EGF profile than that of rOPN and Th-rOPN, which contain both
492 the N-rOPN and C-rOPN fragments, in RB cows. In addition, peptide 1 required larger doses than
493 rOPN to induce a similar effect. The following hypotheses may explain these results: (1) The
494 amino-acid sequences other than the RGD and SVAYGLK motifs might have a supportive role in
495 the normalization of the endometrial EGF profile. (2) The number of amino acids of peptide 1

(Gly151−Lys161, eleven animo-acid residues) is far less than that of rOPN (Leu17−Asn278, 262 animo-acid residues) and, thus, the peptide may be susceptible to denaturation or loss of activity by peptidases present in the vagina [79]. Therefore, we chose higher dose of peptides than that of rOPN. (3) The reason N-rOPN was less effective than rOPN and Th-rOPN may be because the C-terminal end corresponding to peptide 1 of a part of N-rOPN was excessively cleaved by thrombin treatment. In fact, LC-MS/MS analysis indicated that the Th-rOPN solution contained N-rOPN, which lacked a part of the C-terminal amino acids (data not shown).

5. Conclusions

The present study demonstrated that the SVAYGLK motif is the structural element of OPN required to restore the normal endometrial EGF profile and fertility in RB cows. These results also suggest that the RGD motif may play a role in enhancing the effect of the SVAYGLK motif. This knowledge provides a foundation for the elucidation of the mechanism by which OPN regulates endometrial function and for the development of a treatment for improved fertility in RB cows.

CRediT authorship contribution statement

Takashi Tanida: Conceptualization, Data curation, Formal analysis, Funding acquisition, Investigation, Methodology, Visualization, and Writing − original draft. **Takayoshi Tagami**: Conceptualization, Investigation, Methodology, and Writing − review & editing. **Yojiro Yanagawa**: Methodology and Writing - review & editing. **Seiji Katagiri**: Conceptualization, Funding acquisition, Investigation, Methodology, Project administration, Supervision, and Writing − review & editing.

Declarations of interest

None

Acknowledgments

This study was supported by Grants-in-Aid for Scientific Research from the Japan Society for the Promotion of Science (No. 19H00964, 22J20415 and 23H00353), Grants-in-Aid for the Promotion of Livestock Industry from the Japan Racing Association, Grants-in-Aid from the Japan Science and Technology Agency [Support for Pioneering Research Initiated by the Next Generation (SPRING) program (No. JPMJSP2119)], and Grant-in-Aid for Graduate Students from the Ministry of Education, Culture, Sports, Science and Technology [the World-leading Innovative and Smart Education (WISE) Program (No. 1801)]. We acknowledge the support of the farmers and practitioners who have enabled the present study at commercial dairy farms. We thank the Instrumental Analysis Division, Global Facility Center, Creative Research Institution, and Hokkaido University for the use of their amino-acid analyzer, protein sequencer, and LC-MS/MS system to perform amino-acid analysis and providing insight and expertise that greatly assisted the research. We also thank Frontier Institute for their technical assistance.

References

[1] Casida LE. Present status of the repeat-breeder cow problem. J Dairy Sci 1961;44:2323–9. https://doi.org/10.3168/jds.S0022-0302(61)90063-7.

[2] Levine HD. The repeat breeder cow. Bov Pract 1999;33:97–105. https://doi.org/https://doi.org/10.21423/bovine-vol33no2p97-105.

[3] Pérez-Marín CC, Quintela LA. Current insights in the repeat breeder cow syndrome. Animals 2023;13. https://doi.org/10.3390/ani13132187.

[4] Erb RE, Garverick HA, Randel RD, Brown BL, Callahan CJ. Profiles of reproductive hormones associated with fertile and nonfertile inseminations of dairy cows. Theriogenology 1976;5:227–42. https://doi.org/10.1016/0093-691X(76)90235-1.

[5] Kimura M, Nakao T, Moriyoshi M, Kawata K. Luteal phase defeciency as a possible cause of repeat breeding in dairy cows. BritVetJ 1987;143:560–6. https://doi.org/10.1016/0007-1935(87)90047-9.

[6] Shelton K, Gayerie De Abreu MF, Hunter MG, Parkinson TJ, Lamming GE. Luteal inadequacy during the early luteal phase of subfertile cows. J Reprod Fertil 1990;90:1–10. https://doi.org/10.1530/jrf.0.0900001.

[7] Brigstock DR. Growth factors in the uterus: Steroidal regulation and biological actions. Baillieres Clin Endocrinol Metab 1991;5:791–808. https://doi.org/10.1016/S0950-351X(10)80015-1.

[8] Paria BC, Song H, Dey SK. Implantation: Molecular basis of embryo-uterine dialogue. Int J Dev Biol 2001;45:597–605.

[9] Katagiri S, Moriyoshi M. Alteration of the endometrial EGF profile as a potential mechanism connecting the alterations in the ovarian steroid hormone profile to embryonic loss in repeat breeders and high-producing cows. J Reprod Dev 2013;59:415–20. https://doi.org/10.1262/jrd.2013-048.

562 [10] Nelson KG, Takahashi T, Bossert NL, Walmer DK, McLachlan J a. Epidermal growth
563 factor replaces estrogen in the stimulation of female genital-tract growth and
564 differentiation. Proc Natl Acad Sci U S A 1991;88:21–5.
565 https://doi.org/10.1073/pnas.88.1.21.
566 [11] Takatsu K, Kuse M, Yoshioka S, Acosta TJ. Expression of epidermal growth factor (EGF)
567 and its receptor in bovine endometrium throughout the luteal phase: effects of EGF on
568 prostaglandin production in endometrial cells. Anim Reprod 2015;12:328–35.
569 [12] Paria BC, Dey SK. Preimplantation embryo development in vitro: cooperative interactions
570 among embryos and role of growth factors. Proc Natl Acad Sci U S A 1990;87:4756–60.
571 https://doi.org/10.1073/PNAS.87.12.4756.
572 [13] Kliem A, Tetens F, Klonisch T, Grealy M, Fischer B. Epidermal growth factor receptor and
573 ligands in elongating bovine blastocysts. Mol Reprod Dev 1998;51.
574 https://doi.org/10.1002/(sici)1098-2795(199812)51:4<402::aid-mrd7>3.3.co;2-0.
575 [14] Ohtani S, Okuda K, Ohtani M, Yamada J. Immunohistochamically-determined changes in
576 the distribution of insulin-like growth factor-I and epidermal growth factor (EGF) in the
577 bovine endometrium during estrous cycle. J Vet Med Sci 1996;58:1211–7.
578 https://doi.org/10.1292/jvms.58.12_1211.
579 [15] Katagiri S, Moriyoshi M, Takahashi Y. Low incidence of an altered endometrial epidermal
580 growth factor (EGF) profile in repeat breeder Holstein heifers and differential effect of
581 parity on the EGF profile between fertile Holstein (dairy) and Japanese Black (beef) cattle.
582 J Reprod Dev 2013;59:575–9. https://doi.org/10.1262/jrd.2013-067.
583 [16] Badrakh D, Yanagawa Y, Nagano M, Katagiri S. Effect of seminal plasma infusion into the
584 vagina on the normalization of endometrial epidermal growth factor concentrations and
585 fertility in repeat breeder dairy cows. J Reprod Dev 2020;66:149–54.
586 https://doi.org/10.1262/jrd.2019-148.

587 [17] Badrakh D, Shirasawa A, Yanagawa Y, Nagano M, Katagiri S. Identification of bovine
588 seminal plasma proteins with an activity to normalize endometrial epidermal growth factor
589 concentrations in repeat breeder cows. Jpn J Vet Res 2020;68:91–103.
590 https://doi.org/10.14943/jjvr.68.2.91.
591 [18] Kyaw HM, Sato H, Tagami T, Yanagawa Y, Nagano M, Katagiri S. Effects of milk
592 osteopontin on the endometrial epidermal growth factor profile and restoration of fertility in
593 repeat breeder dairy cows. Theriogenology 2022;184:26–33.
594 https://doi.org/10.1016/j.theriogenology.2022.02.008.
595 [19] Tanida T, Tagami T, Sato H, Kwaw HM, Fujikawa T, Nagano M, et al. Effects of
596 recombinant osteopontin expressed in Escherichia coli on the recovery of the endometrial
597 epidermal growth factor profile and fertility in repeat breeder dairy cows. Theriogenology
598 2024;217:159–68. https://doi.org/10.1016/j.theriogenology.2024.01.011.
599 [20] Denhardt DT, Guo X. Osteopontin: a protein with diverse functions. FASEB J
600 1993;7:1475–82. https://doi.org/10.1096/fasebj.7.15.8262332.
601 [21] Icer MA, Gezmen-Karadag M. The multiple functions and mechanisms of osteopontin. Clin
602 Biochem 2018;59:17–24. https://doi.org/10.1016/j.clinbiochem.2018.07.003.
603 [22] Sodek J, Ganss B, Mckeel D. Osteopontin. Crit Rev Oral Biol Med 2000;11:279–303.
604 https://doi.org/https://doi.org/10.1177/10454411000110030101.
605 [23] Brunswig-Spickenheier B, Mukhopadhyay AK. Expression of osteopontin (OPN) mRNA in
606 bovine ovarian follicles and corpora lutea. Reprod Domest Anim 2003;38:175–81.
607 https://doi.org/10.1046/j.1439-0531.2003.00413.x.
608 [24] Poole DH, Ndiaye K, Pate JL. Expression and regulation of secreted phosphoprotein 1 in
609 the bovine corpus luteum and effects on T lymphocyte chemotaxis. Reproduction
610 2013;146:527–37. https://doi.org/10.1530/REP-13-0190.

611 [25] Gabler C, Chapman DA, Killian GJ. Expression and presence of osteopontin and integrins
612 in the bovine oviduct during the oestrous cycle. Reproduction 2003;126:721–9.
613 https://doi.org/10.1530/rep.0.1260721.
614 [26] Johnson GA, Burghardt RC, Spencer TE, Newton GR, Ott TL, Bazer FW. Ovine
615 osteopontin: II. osteopontin and αv β3 integrin expression in the uterus and conceptus
616 during the periimplantation period. Biol Reprod 1999;61:892–9.
617 https://doi.org/10.1095/biolreprod61.4.892.
618 [27] Garlow JE, Ka H, Johnson GA, Burghardt RC, Jaeger LA, Bazer FW. Analysis of
619 osteopontin at the maternal-placental interface in pigs. Biol Reprod 2002;66:718–25.
620 https://doi.org/10.1095/biolreprod66.3.718.
621 [28] Joyce MM, González JF, Lewis S, Woldesenbet S, Burghardt RC, Newton GR, et al.
622 Caprine uterine and placental osteopontin expression is distinct among epitheliochorial
623 implanting species. Placenta 2005;26:160–70.
624 https://doi.org/10.1016/j.placenta.2004.05.009.
625 [29] Erikson DW, Way AL, Chapman DA, Killian GJ. Detection of osteopontin on Holstein bull
626 spermatozoa, in cauda epididymal fluid and testis homogenates, and its potential role in
627 bovine fertilization. Reproduction 2007;133:909–17. https://doi.org/10.1530/REP-06-0228.
628 [30] Lund SA, Giachelli CM, Scatena M. The role of osteopontin in inflammatory processes. J
629 Cell Commun Signal 2009;3:311–22. https://doi.org/10.1007/s12079-009-0068-0.
630 [31] Liu Q, Xie QZ, Zhou Y, Yang J. Osteopontin is expressed in the oviduct and promotes
631 fertilization and preimplantation embryo development of mouse. Zygote 2014;760:622–30.
632 https://doi.org/10.1017/S0967199414000483.
633 [32] Monaco E, Gasparrini B, Boccia L, De Rosa A, Attanasio L, Zicarelli L, et al. Effect of
634 osteopontin (OPN) on in vitro embryo development in cattle. Theriogenology 2009;71:450–
635 7. https://doi.org/10.1016/j.theriogenology.2008.08.012.

[33] Johnson GA, Burghardt RC, Bazer FW, Spencer TE. Osteopontin: Roles in implantation and placentation. Biol Reprod 2003;69:1458–71. https://doi.org/10.1095/biolreprod.103.020651.

[34] Boccia L, Di Francesco S, Neglia G, De Blasi M, Longobardi V, Campanile G, et al. Osteopontin improves sperm capacitation and invitro fertilization efficiency in buffalo (Bubalus bubalis). Theriogenology 2013;80:212–7. https://doi.org/10.1016/j.theriogenology.2013.04.017.

[35] Kuwabara Y, Katayama A, Tomiyama R, Piao H, Kurihara S, Ono S, et al. Gonadotropin regulation and role of ovarian osteopontin in the periovulatory period. J Endocrinol 2015;224:49–59. https://doi.org/10.1530/JOE-14-0203.

[36] Erikson DW, Burghardt RC, Bayless KJ, Johnson GA. Secreted phosphoprotein 1 (SPP1, osteopontin) binds to integrin alphavbeta6 on porcine trophectoderm cells and lntegrin alphavbeta3 on uterine luminal epithelial cells, and promotes trophectoderm cell adhesion and migration. Biol Reprod 2009;81:814–25. https://doi.org/10.1095/biolreprod.109.078600.

[37] Kim J, Erikson DW, Burghardt RC, Spencer TE, Wu G, Bayless KJ, et al. Secreted phosphoprotein 1 binds integrins to initiate multiple cell signaling pathways, including FRAP1/mTOR, to support attachment and force-generated migration of trophectoderm cells. Matrix Biol 2010;29:369–82. https://doi.org/10.1016/j.matbio.2010.04.001.

[38] Weber GF, Zawaideh S, Hikita S, Kumar VA, Cantor H, Ashkar S. Phosphorylation-dependent interaction of osteopontin with its receptors regulates macrophage migration and activation. J Leukoc Biol 2002;72:752–61. https://doi.org/10.1189/jlb.72.4.752.

[39] Minai-Tehrani A, Chang SH, Park SB, Cho MH. The O-glycosylation mutant osteopontin alters lung cancer cell growth and migration in vitro and in vivo. Int J Mol Med 2013;32:1137–49. https://doi.org/10.3892/ijmm.2013.1483.

661 [40] Ashkar S, Weber GF, Panoutsakopoulou V, Sanchirico ME, Jansson M, Zawaideh S, et al.
662 Eta-1 (osteopontin): An early component of type-1 (cell-mediated) immunity. Science (80-)
663 2000;287:860–4. https://doi.org/10.1126/science.287.5454.860.
664 [41] Sahdev S, Khattar SK, Saini KS. Production of active eukaryotic proteins through bacterial
665 expression systems: A review of the existing biotechnology strategies. Mol Cell Biochem
666 2008;307:249–64. https://doi.org/10.1007/s11010-007-9603-6.
667 [42] Senger DR, Ledbetter SR, Claffey KP, Papadopoulos-Sergiou A, Perruzzi CA, Detmar M.
668 Stimulation of endothelial cell migration by vascular permeability factor/vascular
669 endothelial growth factor through cooperative mechanisms involving the α(v)β3 integrin,
670 osteopontin, and thrombin. Am J Pathol 1996;149:293–305.
671 [43] Yamamoto N, Sakai F, Kon S, Morimoto J, Kimura C, Yamazaki H, et al. Essential role of
672 the cryptic epitope SLAYGLR within osteopontin in a murine model of rheumatoid
673 arthritis. J Clin Invest 2003;112:181–8. https://doi.org/10.1172/JCI17778.
674 [44] Sørensen ES, Petersen TE, Højrup P. Posttranslational modifications of bovine osteopontin:
675 Identification of twenty-eight phosphorylation and three O-glycosylation sites. Protein Sci
676 1995;4:2040–9. https://doi.org/10.1002/pro.5560041009.
677 [45] Lin YH, Yang-Yen HF. The osteopontin-CD44 survival signal involves activation of the
678 phosphatidylinositol 3-kinase/akt signaling pathway. J Biol Chem 2001;276:46024–30.
679 https://doi.org/10.1074/jbc.M105132200.
680 [46] Christensen B, Sørensen ES. Structure , function and nutritional potential of milk
681 osteopontin. Int Dairy J 2016;57:1–6. https://doi.org/10.1016/j.idairyj.2016.02.034.
682 [47] Mezu-Ndubuisi OJ, Maheshwari A. The role of integrins in inflammation and angiogenesis.
683 Pediatr Res 2021;89:1619–26. https://doi.org/10.1038/s41390-020-01177-9.
684 [48] Sørensen ES, Christensen B. Milk osteopontin and human health. Nutrients 2023;15.
685 https://doi.org/10.3390/nu15112423.

686 [49] Yokosaki Y, Matsuura N, Sasaki T, Murakami I, Schneider H, Higashiyama S, et al. The
687 integrin α9β1 binds to a novel recognition sequence (SVVYGLR) in the thrombin-cleaved
688 amino-terminal fragment of osteopontin. J Biol Chem 1999;274:36328–34.
689 https://doi.org/10.1074/jbc.274.51.36328.
690 [50] Barry ST, Ludbrook SB, Murrison E, Horgan CMT. Analysis of the α4β1 integrin-
691 osteopontin interaction. Exp Cell Res 2000;258:342–51.
692 https://doi.org/10.1006/excr.2000.4941.
693 [51] Bayless KJ, Davis GE. Identification of dual α4β1 integrin binding sites within a 38 amino
694 acid domain in the N-terminal thrombin fragment of human osteopontin. J Biol Chem
695 2001;276:13483–9. https://doi.org/10.1074/jbc.M011392200.
696 [52] Luo Y, Matejic T, Ng CK, Nunnally B, Porter T, Raso S, et al. Characterization and
697 analysis of biopharmaceutical proteins. Sep Sci Technol 2011;10:283–359.
698 https://doi.org/10.1016/B978-0-12-375680-0.00008-5.
699 [53] Perkins DN, Pappin DJC, Creasy DM, Cottrell JS. Probability-based protein identification
700 by searching sequence databases using mass spectrometry data. Electrophoresis
701 1999;20:3551–67. https://doi.org/10.1002/(SICI)1522-2683(19991201)20:18<3551::AID-
702 ELPS3551>3.0.CO;2-2.
703 [54] Ikeuchi M, Takio K, Inoue Y. N-terminal sequencing of photosystem II low-molecular-
704 mass proteins 5 and 4.1 kDa components of the O2-evolving core complex from higher
705 plants. FEBS Lett 1989;242:263–9. https://doi.org/10.1016/0014-5793(89)80482-X.
706 [55] Mizuno T, Mori H, Ito H, Matsui H, Kimura A, Chiba S. Molecular cloning of isomaltotrio-
707 dextranase gene from Brevibacterium fuscum var. dextranlyticum strain 0407 and its
708 expression in Escherichia coli. Biosci Biotechnol Biochem 1999;63:1582–8.
709 https://doi.org/10.1271/bbb.63.1582.

710 [56] Noble JE, Bailey MJA. Quantitation of protein. Methods Enzymol 2009;463:73–95.
711 https://doi.org/10.1016/S0076-6879(09)63008-1.
712 [57] Mee JF, Buckley F, Ryan D, Dillon P. Pre-breeding ovaro-uterine ultrasonography and its
713 relationship with first service pregnancy rate in seasonal-calving dairy herds. Reprod
714 Domest Anim 2009;44:331–7. https://doi.org/10.1111/j.1439-0531.2008.01079.x.
715 [58] Dubuc J, Duffield TF, Leslie KE, Walton JS, LeBlanc SJ. Definitions and diagnosis of
716 postpartum endometritis in dairy cows. J Dairy Sci 2010;93:5225–33.
717 https://doi.org/10.3168/jds.2010-3428.
718 [59] Wiltbank MC, Pursley JR. The cow as an induced ovulator : Timed AI after synchronization
719 of ovulation. Theriogenology 2014;81:170–85.
720 https://doi.org/10.1016/j.theriogenology.2013.09.017.
721 [60] Katagiri S, Takahashi Y. Changes in EGF concentrations during estrous cycle in bovine
722 endometrium and their alterations in repeat breeder cows. Theriogenology 2004;62.
723 https://doi.org/10.1016/j.theriogenology.2003.08.019.
724 [61] Katagiri S, Takahashi Y. Potential relationship between normalization of endometrial
725 epidermal growth factor profile and restoration of fertility in repeat breeder cows. Anim
726 Reprod Sci 2006;95:54–66. https://doi.org/10.1016/j.anireprosci.2005.09.001.
727 [62] Katagiri S, Moriyoshi M, Yanagawa Y. Endometrial epidermal growth factor profile and its
728 abnormalities in dairy cows. J Reprod Dev 2016;62:465–70.
729 https://doi.org/10.1262/jrd.2016-039.
730 [63] Benjamini Y, Hochberg Y. Controlling the false discovery rate : A practical and powerful
731 approach to multiple testing. J R Stat Soc Ser B 1995;57:289–300.
732 [64] Smith LL, Giachelli CM. Structural requirements for α9β1-mediated adhesion and
733 migration to thrombin-cleaved osteopontin. Exp Cell Res 1998;242:351–60.
734 https://doi.org/10.1006/excr.1998.4108.

[65] Wu G, Li X, Seo H, McLendon BA, Kramer AC, Bazer FW, et al. Osteopontin (OPN)/secreted phosphoprotein 1 (SPP1) binds integrins to activate transport of ions across the porcine placenta. Front Biosci - Landmark 2022;27:117. https://doi.org/10.31083/j.fbl2704117.

[66] Hui T, Sørensen ES, Rittling SR. Osteopontin binding to the alpha 4 integrin requires highest affinity integrin conformation, but is independent of post-translational modifications of osteopontin. Matrix Biol 2015;41:19–25. https://doi.org/10.1016/j.matbio.2014.11.005.

[67] Odhiambo JF, Poole DH, Hughes L, DeJarnette JM, Inskeep EK, Dailey RA. Pregnancy outcome in dairy and beef cattle after artificial insemination and treatment with seminal plasma or transforming growth factor beta-1. Theriogenology 2009;72:566–71. https://doi.org/10.1016/j.theriogenology.2009.04.013.

[68] Ortiz WG, Rizo JA, Carvalheira LR, Ahmed BMS, Estrada-Cortes E, Harstine BR, et al. Effects of intrauterine infusion of seminal plasma at artificial insemination on fertility of lactating Holstein cows. J Dairy Sci 2019;102:6587–94. https://doi.org/10.3168/jds.2019-16251.

[69] Fernandez-Fuertes B. Review: The role of male reproductive tract secretions in ruminant fertility. Animal 2023;17:100773. https://doi.org/10.1016/j.animal.2023.100773.

[70] Murphy EM, Kelly AK, O'Meara C, Eivers B, Lonergan P, Fair S. Influence of bull age, ejaculate number, and season of collection on semen production and sperm motility parameters in holstein friesian bulls in a commercial artificial insemination centre. J Anim Sci 2018;96:2408–18. https://doi.org/10.1093/jas/sky130.

[71] Perkins JR, Olds D, Seath DM. A Study of 1,000 Bovine Genitalia. J Dairy Sci 1954;37:1158–63. https://doi.org/10.3168/jds.S0022-0302(54)91384-3.

[72] Suarez SS, Pacey AA. Sperm transport in the female reproductive tract. Hum Reprod Update 2006;12:23–37. https://doi.org/10.1093/humupd/dmi047.

[73] Campanile G, Baruselli PS, Limone A, D'Occhio MJ. Local action of cytokines and immune cells in communication between the conceptus and uterus during the critical period of early embryo development, attachment and implantation – Implications for embryo survival in cattle: A review. Theriogenology 2021;167:1–12. https://doi.org/10.1016/j.theriogenology.2021.02.020.

[74] Gori I, Pellegrini C, Staedler D, Russell R, Jan C, Canny GO. Tumor necrosis factor-α activates estrogen signaling pathways in endometrial epithelial cells via estrogen receptor α. Mol Cell Endocrinol 2011;345:27–37. https://doi.org/10.1016/j.mce.2011.06.043.

[75] Huet-Hudson YM, Chakrabortyt C, De SK, Suzuki Y, Andrews GK, Dey SK. Estrogen regulates the synthesis of epidermal growth factor in mouse uterine epithelial cells. Mol Endocrinol 1990;4:510–23. https://doi.org/10.1210/mend-4-3-510.

[76] Kourepini E, Aggelakopoulou M, Alissafi T, Paschalidis N, Simoes DCM, Panoutsakopoulou V. Osteopontin expression by CD103- dendritic cells drives intestinal inflammation. Proc Natl Acad Sci U S A 2014;111. https://doi.org/10.1073/pnas.1316447111.

[77] Johnson GA, Burghardt RC, Bazer FW, Seo H, Cain JW. Integrins and their potential roles in mammalian pregnancy. J Anim Sci Biotechnol 2023;14:1–19. https://doi.org/10.1186/s40104-023-00918-0.

[78] Wing TT, Erikson DW, Burghardt RC, Bazer FW, Bayless KJ, Johnson GA. OPN binds alpha V integrin to promote endothelial progenitor cell incorporation into vasculature. Reproduction 2020;159:465–78. https://doi.org/10.1530/REP-19-0358.

[79] Hussain A, Ahsan F. The vagina as a route for systemic drug delivery. J Control Release 2005;103:301–13. https://doi.org/10.1016/j.jconrel.2004.11.034.

784

Table 1. Effect of Th-rOPN, N-rOPN, and C-rOPN on the restoration of the normal endometrial epidermal growth factor (EGF) profile in repeat breeder cows.

Samples	(n)	No. (%) of cows with the normal endometrial EGF profile after treatment	No. of cows subjected to pregnancy diagnosis on days 30-35	No. (%) of cows conceived
rOPN	(18)	10 (55.6) [A]	16	8 (50.0)
Th-rOPN	(14)	9 (64.3) [A]	12	5 (41.7)
N-rOPN	(20)	5 (25.0) [AB]	20	6 (30.0)
C-rOPN	(13)	1 (7.7) [B]	12	4 (33.3)

rOPN: Recombinant osteopontin, Th-rOPN: the mixture of fragments generated by thrombin cleavage of rOPN, N-rOPN: N-terminal fragments generated by thrombin cleavage of rOPN, C-rOPN: C-terminal fragments generated by thrombin cleavage of rOPN. Doses of rOPN, N-rOPN and C-rOPN were 16 nmol. The dose of Th-rOPN was fragments generated by 16 nmol of rOPN. [A,B] Proportions in a same column differ significantly ($P < 0.05$).

Table 2. Effect of osteopontin (OPN) peptides on the restoration of the normal endometrial epidermal growth factor (EGF) profile in repeat breeder cows.

Samples	Dose	Trail 1		Trial 2		Total	
		No. of cows treated	No. (%) of cows with the normal endometrial EGF profile after treatment	No. of cows treated	No. (%) of cows with the normal endometrial EGF profile after treatment	No. of cows treated	No. (%) of cows with the normal endometrial EGF profile after treatment
PBS	−	45	7 (15.6) [a]	30	9 (30.0)	75	16 (21.3) [A]
rOPN	9.5 nmol	83	53 (63.9) [b]	28	15 (53.6)	111	68 (61.3) [B]
Peptide 1	32 nmol	25	8 (32.0) [†]	–	–	–	–
	320 nmol	25	13 (52.0) [*]	25	15 (60.0)	50	28 (56.0) [B]
	1600 nmol	25	11 (44.0) [*]	25	15 (60.0)	50	26 (52.0) [B]
Peptide 2	320 nmol	20	4 (20.0) [†]	–	–	–	–
	1600 nmol	20	5 (25.0) [†]	–	–	–	–
Peptide 3	320 nmol	25	9 (36.0) [†]	–	–	–	–
	1600 nmol	23	13 (56.5) [*]	32	15 (46.9)	55	28 (50.9) [B]

rOPN: Recombinant OPN, Peptide 1: the GRGDSVAYGLK peptide, Peptide 2: the GRGDS peptide, Peptide 3: the SVAYGLK peptide. [*, †] Proportions of cows with the normal endometrial EGF profile after treatment of peptide 1, peptide 2, and peptide 3 groups were compared to those of PBS (negative control) and rOPN (positive control) groups in trial 1 and 2. Asterisks (*) and daggers (†) indicate the values differ from the PBS and rOPN groups, respectively ($P < 0.05$). [a, b] Proportions differ between PBS and rOPN groups in a same column ($P < 0.05$). [A,B] Proportion of cows with the normal

endometrial EGF profile after treatment of PBS, rOPN, peptide 1 (320 and 1,600 nmol) and peptide 3 (1,600 nmol) groups were calculated and compared between groups in total of trials. The proportions with different uppercase letters differ significantly in a same column ($P < 0.05$).

20 Table 3. Effect of osteopontin (OPN) peptides on the restoration of fertility in repeat breeder cows.

Samples	Dose	Endometrial EGF profile after treatment	Trial 1		Trial 2		Total of trials	
			No. of cows subjected to pregnancy diagnosis on days 30-35	No. (%) of cows conceived	No. of cows subjected to pregnancy diagnosis on days 30-35	No. (%) of cows conceived	No. of cows subjected to pregnancy diagnosis on days 30-35	No. (%) of cows conceived
PBS	–	Normalized	7	4 (57.1) [C]	9	5 (55.6)	16	9 (56.3) [C]
		Unnormalized	37	3 (8.1) [D]	21	4 (19.0)	58	7 (12.1) [D]
		Total	44	7 (15.9) [a]	30	9 (30.0)	74	16 (21.6) [A]
rOPN	9.5 nmol	Normalized	52	33 (63.5) [C]	15	10 (66.7) [C]	67	43 (64.2) [C]
		Unnormalized	29	6 (20.7) [D]	13	3 (23.1) [D]	42	9 (21.4) [D]
		Total	81	39 (48.1) [b]	28	13 (46.4)	109	52 (47.7) [B]
Peptide 1	32 nmol	Normalized	8	3 (37.5)	–	–	–	–
		Unnormalized	17	2 (11.8)	–	–	–	–
		Total	25	5 (20.0)	–	–	–	–
	320 nmol	Normalized	13	9 (69.2) [C]	15	9 (60.0)	28	18 (64.3) [C]
		Unnormalized	12	2 (16.7) [D]	10	2 (20.0)	22	4 (18.2) [D]
		Total	25	11 (44.0) [*]	25	11 (44.0)	50	22 (44.0) [B]
	1600 nmol	Normalized	11	6 (54.5)	15	11 (73.3) [C]	26	17 (65.4) [C]
		Unnormalized	14	6 (42.9)	10	2 (20.0) [D]	24	8 (33.3) [D]
		Total	25	12 (48.0) [*]	25	13 (52.0)	50	25 (50.0) [B]
Peptide 2	320 nmol	Normalized	4	3 (75.0) [C]	–	–	–	–
		Unnormalized	15	1 (6.7) [D]	–	–	–	–
		Total	19	4 (21.1)	–	–	–	–
	1600 nmol	Normalized	5	3 (60.0)	–	–	–	–
		Unnormalized	15	3 (20.0)	–	–	–	–
		Total	20	6 (30.0)	–	–	–	–
Peptide 3	320 nmol	Normalized	9	7 (77.8) [C]	–	–	–	–
		Unnormalized	16	3 (18.8) [D]	–	–	–	–
		Total	25	10 (40.0)	–	–	–	–
	1600 nmol	Normalized	13	8 (61.5)	15	10 (66.7) [C]	28	18 (64.3) [C]
		Unnormalized	10	2 (20.0)	17	3 (17.6) [D]	27	5 (18.5) [D]
		Total	23	10 (43.5) [*]	32	13 (40.6)	55	23 (41.8) [B]

rOPN: Recombinant OPN, Peptide 1: the GRGDSVAYGLK peptide, Peptide 2: the GRGDS peptide, Peptide 3: the SVAYGLK peptide. EGF: epidermal growth factor. * Conception rates of peptide 1, peptide 2, and peptide 3 groups were compared to those of PBS (negative control) and rOPN (positive control) groups in trial 1 and 2. Asterisks (*) indicate the values differ from the PBS group, respectively ($P < 0.05$). [a, b] Conception rates differ significantly between PBS and rOPN groups in a same column ($P < 0.05$). [A, B] Overall conception rates of cows of PBS, rOPN, peptide 1 (320 and 1,600 nmol), and peptide 3 (1,600 nmol) groups were calculated and compared between groups in total of trials. The conception rates with different uppercase letters differ significantly in a same column ($P < 0.05$). [C, D] Proportions differ significantly between the different endometrial EGF profile within a same group ($P < 0.05$).

29 Table 4. Effect of the peptide 4 on the restoration of the normal endometrial epidermal growth factor

30 (EGF) profile in repeat breeder cows.

31

Samples	Dose	(n)	No. (%) of cows with the normal endometrial EGF profile after treatment	No. of cows subjected to pregnancy diagnosis on days 30-35	No. (%) of cows conceived
PBS	−	(24)	4 (16.7) [A]	24	5 (20.8)
Peptide 1	320 nmol	(78)	35 (44.9) [B]	78	31 (39.7)
Peptide 4	320 nmol	(50)	8 (16.0) [A]	50	10 (20.0)
	1600 nmol	(26)	5 (19.2) [A]	26	8 (30.8)

32

33 Peptide 1: the GRGDSVAYGLK peptide. Peptide 4: the GRGESVAYGLK peptide. [A, B] Proportions

34 differ significantly in a same column ($P < 0.05$).

35

Fig. 1.

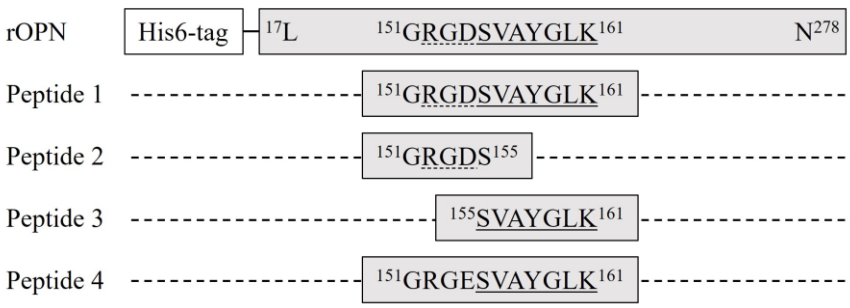
rOPN
His6-tag
17L
151GRGDSVAYGLK161
N278
Peptide 1
151GRGDSVAYGLK161
Peptide 2
151GRGDS155
Peptide 3
155SVAYGLK161
Peptide 4
151GRGESVAYGLK161

Fig. 2.

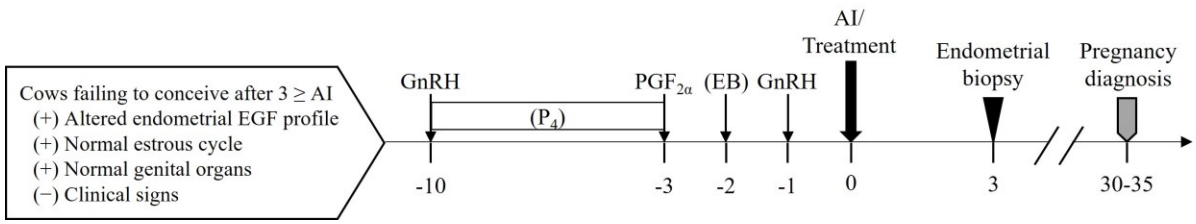
Cows failing to conceive after 3 ≥ AI
(+) Altered endometrial EGF profile
(+) Normal estrous cycle
(+) Normal genital organs
(−) Clinical signs
GnRH
(P4)
PGF2α
(EB)
GnRH
AI/
Treatment
Endometrial
biopsy
Pregnancy
diagnosis
-10
-3
-2
-1
0
3
30-35

Fig. 3.

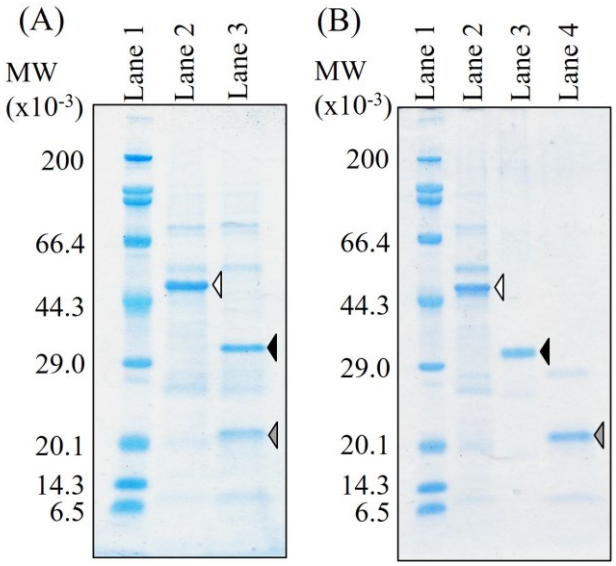

(C)

N-rOPN (black-arrowed fragment)

*MRIAVICFCLLGIASALPVKPTSSGSSEEK***QLNNKY**
PDAVATWLKPDPSQKQTFLAPQNSVSSEETDD
NKQNTLPSK*SNESPEQTDDLDDDDDNSQDVNSN*
DSDDAETTDDPDHSDESHHSDESDEVDFPTDIPTI
AVFTPFIPTESANDGRGDSVAYGLKSR

C-rOPN (gray-arrowed fragment)

*SKKFR***RS****NVQSPDATEEDFTSHIESEEMHDAP**
KKTSQLTDHSKETNSSELSK*ELTPKAK***DKNKH**
SNLIESQENSKL*SQEFHSLEDKLDLDHKSEEDKH*
*LK***IRISHELDSASSEVN**

Fig. 4.

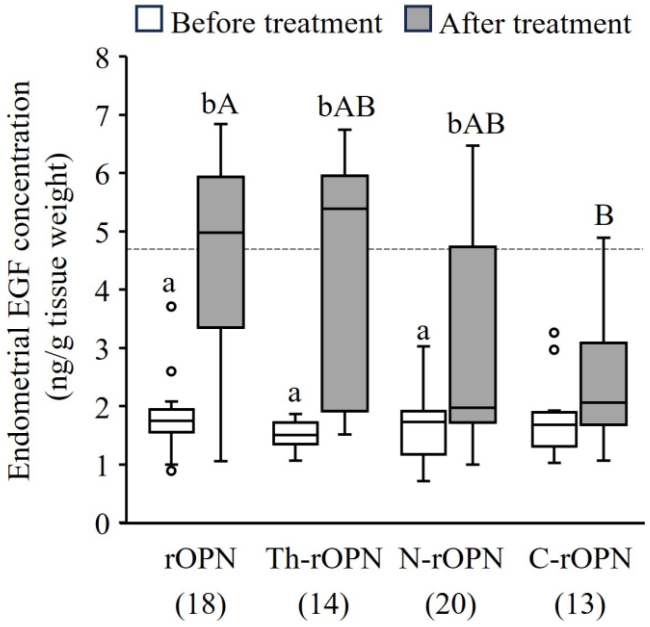
Before treatment
After treatment
Endometrial EGF concentration (ng/g tissue weight)
0
1
2
3
4
5
6
7
8
a
bA
a
bAB
a
bAB
B
rOPN (18)
Th-rOPN (14)
N-rOPN (20)
C-rOPN (13)

Fig. 5.

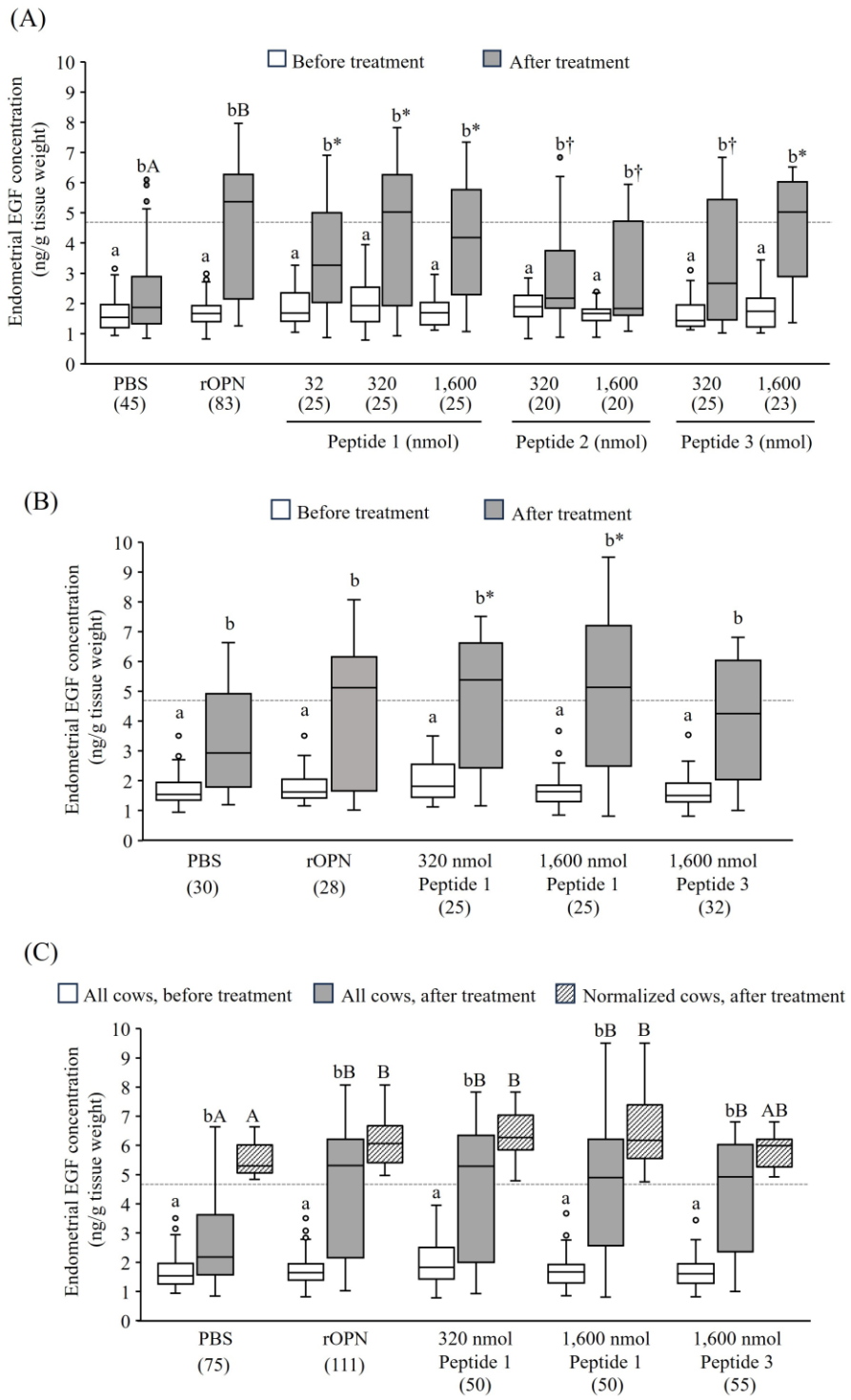
(A)
Before treatment
After treatment
Endometrial EGF concentration (ng/g tissue weight)
PBS (45)
rOPN (83)
32 (25)
320 (25)
1,600 (25)
320 (20)
1,600 (20)
320 (25)
1,600 (23)
Peptide 1 (nmol)
Peptide 2 (nmol)
Peptide 3 (nmol)
(B)
Before treatment
After treatment
Endometrial EGF concentration (ng/g tissue weight)
PBS (30)
rOPN (28)
320 nmol Peptide 1 (25)
1,600 nmol Peptide 1 (25)
1,600 nmol Peptide 3 (32)
(C)
All cows, before treatment
All cows, after treatment
Normalized cows, after treatment
Endometrial EGF concentration (ng/g tissue weight)
PBS (75)
rOPN (111)
320 nmol Peptide 1 (50)
1,600 nmol Peptide 1 (50)
1,600 nmol Peptide 3 (55)

Fig. 6

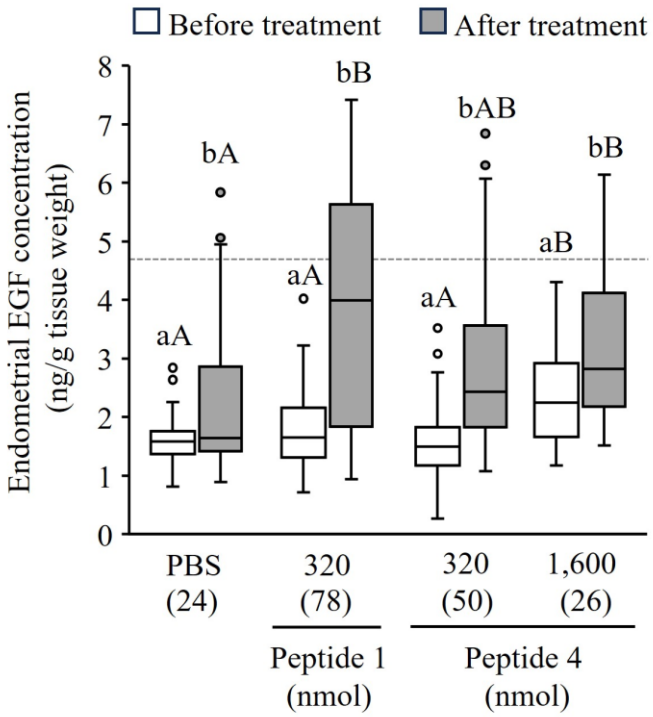
Before treatment
After treatment
Endometrial EGF concentration (ng/g tissue weight)
0
1
2
3
4
5
6
7
8
aA
bA
aA
bB
aA
bAB
aB
bB
PBS (24)
320 (78)
320 (50)
1,600 (26)
Peptide 1 (nmol)
Peptide 4 (nmol)

Figure captions

Fig. 1. A schematic structure of the recombinant osteopontin (OPN) and OPN peptides.
Recombinant OPN (rOPN) was expressed in *Escherichia. coli* as an N-terminally His6-tagged recombinant protein. The amino-acid sequences of peptide 1, peptide 2, and peptide 3 were designed to correspond to Gly151−Lys161, Gly151−Ser155, and Ser155−Lys161 of bovine OPN, respectively. Dashed and solid underlined sections indicate the RGD (Arg152−Asp154) and SVAYGLK (Ser155−Lys161) motifs, respectively. Peptide 4 was a peptide 1 with the aspartic acid (D) replaced with glutamic acid (E).

Fig. 2. The outline of activities.
Before enrollment in the study, repeat breeder (RB) cows were recruited by the criteria described in the figure. They were examined for the epidermal growth factor (EGF) profile by a single examination of the endometrial EGF concentration on day 3. Those showing an altered endometrial EGF profile were used for further study. They were synchronized for ovulation and subjected to AI 16−20 h after the second gonadotropin-releasing hormone (GnRH) treatment of the ovulatory synchronization protocol (day 0). Immediately after AI, the cows were infused with treatment samples into the vagina. The endometrial EGF concentration was determined for a second time on day 3, and pregnancy was diagnosed 30–35 days after AI. P_4: progesterone; $PGF_{2\alpha}$: prostaglandin $F_{2\alpha}$; EB: estradiol benzoate.

Fig. 3. Recombinant proteins for the infusion study.
Sodium dodecyl-sulfate polyacrylamide gel electrophoresis (SDS-PAGE) was performed to the recombinant protein preparations. White arrowhead: the recombinant osteopontin (rOPN) identified by western blotting [23]. Black and gray arrowheads: N-terminal (N-rOPN) and C-terminal (C-rOPN) fragments of rOPN cleaved by thrombin determined by peptide-mass

fingerprinting (PMF). (A) Lane 1, molecular mass marker. Lane 2, rOPN preparation. Lane 3, thrombin-cleaved rOPN (Th-rOPN) preparation. (B) Lane 1, molecular mass marker. Lane 2, rOPN preparation. Lane 3 and 4, Th-rOPN fragments separated on a benzamidine column: the bound and unbound fraction, respecetively. (C) Protein sequence coverage of N-rOPN and C-rOPN determined by PMF. The amino acids covered by the analysis are indicated with bold characters and a solid underline. Seven amino-acid residues in C-rOPN fragment shown in light shading were determined by N-terminal amino-acid sequence analysis of the fragment indicated with a gray arrowhead.

Fig. 4. The effect of Th-rOPN, N-rOPN, and C-rOPN on the endometrial epidermal growth factor (EGF) concentrations in repeat breeder (RB) cows.
rOPN: Recombinant osteopontin, Th-rOPN: the mixture of fragments generated by thrombin cleavage of rOPN, N-rOPN: N-terminal fragments generated by thrombin cleavage of rOPN, C-rOPN: C-terminal fragments generated by thrombin cleavage of rOPN. Doses of rOPN, N-rOPN and C-rOPN were 16 nmol. The dose of Th-rOPN was fragments generated by 16 nmol of rOPN. The gray dot line indicates the threshold concentration of the normal endometrial EGF profile (4.7 ng/g tissue weight). Numbers in parenthesis below each samples indicate the number of cows for each group. $^{a, b}$ Values differ before and after treatment within the same group ($P < 0.05$). $^{A, B}$ Values between groups differ after treatment ($P < 0.05$).

Fig. 5. The effect of osteopontin (OPN) peptides on the endometrial epidermal growth factor (EGF) concentrations in repeat breeder (RB) cows in trial 1 (A), trial 2 (B), and combined data from the two trials (C) for Study 2.
rOPN: recombinant OPN. Peptide 1: the GRGDSVAYGLK peptide. Peptide 2: the GRGDS peptide. Peptide 3: the SVAYGLK peptide. The gray dot line indicates the threshold concentration

of the normal endometrial EGF profile (4.7 ng/g tissue weight). Numbers in parenthesis below each samples indicate the number of cows for each group. (A) Asterisks (*) and daggers (†) indicate the values differ from the PBS and rOPN groups, respectively ($P < 0.05$). $^{a, b}$ Values differ before and after treatment within the same group ($P < 0.05$,). $^{A, B}$ Values in the PBS and rOPN groups differ after treatment ($P < 0.05$). (B) Asterisks (*) indicate the values differ from the PBS group ($P < 0.05$). $^{a, b}$ Values differ before and after treatment within the same group ($P < 0.05$). (C) $^{a, b}$ Values differ before and after treatment within all cows of the same group ($P < 0.05$). $^{A, B}$ Values between groups differ within all cows or cows with a normalized EGF profile (normalized cows) after treatment ($P < 0.05$).

Fig. 6. The effect of peptide 4 on the endometrial epidermal growth factor (EGF) concentrations in repeat breeder (RB) cows.

Peptide 1: the GRGDSVAYGLK peptide. Peptide 4: the GRGESVAYGLK peptide. The gray dot line indicates the threshold concentration of the normal endometrial EGF profile (4.7 ng/g tissue weight). Numbers in parenthesis below each samples indicate the number of cows for each group. $^{a, b}$ Values differ between before and after treatment within the same group ($P < 0.05$). $^{A, B}$ Values differ between groups before and after treatment ($P < 0.05$).